Hydrogen-Bond Interactions between Ester and Urethane Linkages in Small Model Compounds and Polyurethanes

Fu-Sen Yen and Jin-Long Hong*

Department of Materials Science and Engineering, National Sun Yat-Sen University, Kaohsiung, Taiwan 80424, R.O.C.

Received June 19, 1997; Revised Manuscript Received September 29, 1997[⊗]

ABSTRACT: Four model compounds (U_s, U_u, UE_{ex}, and UE_{in}) and two polyurethanes (PU_1 and PU_2) were prepared to monitor the hydrogen-bond (H-bond) interactions of urethane−urethane and urethane−ester (including external and internal esters). The results from differential scanning calorimetry (DSC) and X-ray diffraction suggested that the infrared absorption patterns in the −NH and −C═O regions are closely related to the thermal history of the test specimen. Except for the incapability of the internal ester −C═O to form an H-bond with urethane −NH, five −C═O absorption bands can be assigned and attributed to free internal ester, free urethane, free external ester, bonded external ester, and disordered and ordered bonded urethane absorptions. The frequencies of the respective −C═O band maxima obtained from the model compounds were given. In cases of polyurethanes, the −C═O absorption of the amorphous PU_1 was assigned on the basis of the deconvoluted result of a heat-treated UE_{ex}, while the liquid crystalline PU_2 has its −C═O absorptions assigned on the basis of the physical states of the test specimen. The as-reacted PU_2 has its −C═O absorptions closely related to the heat-treated UE_{in}; however, as PU_2 was heated into the mesophase, the orientation order caused the corresponding −C═O absorptions similar to those for the as-reacted UE_{in}.

Introduction

Polyurethanes have gained lots of attention due to their fascinating hydrogen-bond (H-bond) behavior.[1,2] The urethane linkages in homopolyurethanes can serve as H-bond acceptor and donor. In polyether−polyurethane (PEPU) segmented block copolymers, the urethane −NH can bond to either the polyether −O− linkage or the urethane −C═O groups. For the case of polyester−polyurethane (PEsPU) segmented block copolymers (or ester-based polyurethanes), more complications arise since both the ester and urethane carbonyl groups are the potential H-bond acceptors, which consequently obscure the −C═O absorption patterns and add analysis difficulty in this region.

The infrared (IR) spectrometer is a powerful instrument for the investigation of the H-bond behavior in polyurethanes. To probe for the complicated interactions, small molecules with urethane groups can serve as model compounds to simulate the complicated interactions in large macromolecules. An IR study on the solution of model ethyl phenyl carbamate (EP, C_6H_5-$NHCOOC_2H_5$)[3] in CCl_4 revealed its free and bonded −NH (−NH_{free} and −NH_{bonded}) stretchings located at 3447 and 3339 cm^{-1}, respectively. Upon addition of dibutyl ether (DE), the −NH_{free} band remained intact while the −NH_{bonded} one moved to 3297 cm^{-1}. The shift of the −NH_{bonded} band to a lower frequency was caused by the interaction between the urethane −NH in EP and the −O− linkage in DE. Analogously, the urethane−ester interaction had been studied by adding dimethyl adipate (DA) to the model EP solution.[4] The corresponding spectrum also showed the inertness of the −NH_{free} band, but for the −NH_{bonded}, it shifted to a lower frequency of 3363 cm^{-1}. The two results shown above suggest that the urethane−ether interactions are stronger than the urethane−ester ones. A study on the solution of EP in CCl_4 gave the data of the free and bonded urethane carbonyl (−$C═O_{free,u}$ and −$C═O_{bonded,u}$) absorptions at 1740 and 1710 cm^{-1}, respectively. As for the effect of additives (DE or DA), no data on the carbonyl absorption were given. Solution IR spectra of model compounds synthesized from 2,4- (and 2,6-) TDI with *n*-BuOH[5] exhibited the −NH_{free}, −NH_{bonded}, and −$C═O_{free,u}$ absorptions at the same frequencies but for the −$C═O_{bonded,u}$, 1720 and 1700 cm^{-1} were assigned for compounds from 2,4- and 2,6-TDI, respectively. The related solid state IR spectra for the 2,6-TDI/MeOH system[6] revealed only one ordered −$C═O_{bonded,u}$ absorption centered at 1699 cm^{-1}. For the comparative 2,4-TDI case, two urethane −C═O bands at 1716 and 1699 cm^{-1} were observed and assigned to be disordered and ordered −$C═O_{bonded,u}$ absorptions, respectively. A lower absorption frequency of band maximum was generally observed for compounds in the solid state as compared to the solution case.

Homopolyurethanes, PEPU, and PEsPU segmented block copolymers had been previously investigated. PEPU films prepared from 2,4-TDI (and 2,6-TDI) and butanediol/poly(tetramethylene oxide)[7] have their −NH_{free} (3460 cm^{-1}), −NH_{bonded} (3320 and 3300 cm^{-1}), −$C═O_{free,u}$ (1740 cm^{-1}), and −$C═O_{bonded,u}$ (1720 and 1700 cm^{-1}) stretching frequencies approximately correlated with those obtained from the model compounds cited above. Liquid crystalline polyurethane (LCPU)[5,8] prepared from mesogenic diol, bis(6-hydroxyhexyl)biphenyl, BP_6, and 2,4-TDI illustrated the morphological effect on the infrared spectra. The carbonyl absorption bands (−$C═O_{free,u}$ at 1731 and −$C═O_{bonded,u}$ at 1707 cm^{-1}) were broad for the as-reacted LCPU. After annealing at high temperature, LCPU had its −$C═O_{free,u}$ absorption shifted to 1735 cm^{-1} while for the −$C═O_{bonded,u}$ band, two resolved peaks corresponding to the disordered and ordered −$C═O_{bonded,u}$ absorptions were observed at around 1714−1716 and 1699−1695 cm^{-1}, respectively. Also, a study had been performed on polyurethane prepared from BP_6 and 2,5-TDI and similar results were obtained.[9] Liquid crystalline PEPU segmented block copolymers with BP_6/TDI as the hard segment and PTMO as the soft segment were also prepared and studied.[10] Application of IR spectroscopy revealed that the elastic deformation induced the rear-

[⊗] Abstract published in *Advance ACS Abstracts,* November 15, 1997.

S0024-9297(97)00898-X CCC: $14.00

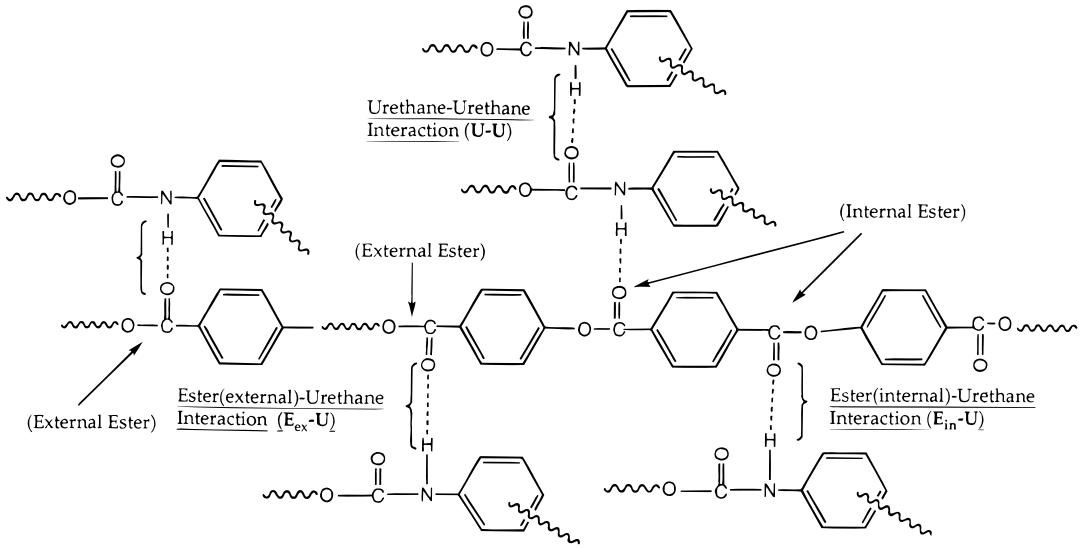

Figure 1. Possible H-bond pairs between esters (either internal or external ester) and urethanes.

rangement of some hard segments in the mesophase into a more ordered packing. Other IR studies in polyurethanes[11−18] were mostly concentrated on the polyether-based systems; few were on the polyester-based systems. An IR study of PEsPU prepared from 2,4-TDI and poly(ethylene adipate) glycol was previously described.[4] The $-NH_{free}$ absorption was reported to appear at 3450 cm^{-1}, but no data on the carbonyl region were given. Another result from PEsPU prepared from poly(tetramethylene adipate), methylenediphenyl diisocyanate (MDI), and 1,4-butanediol[6] suggested that the $-NH_{bonded}$ absorption occurs at 3320 cm^{-1} but for the −C═O mode, a complicated absorption pattern in the ranges of 1750 and 1700 cm^{-1} was claimed. Other reports in this category, including the segmented poly(ester-urethane)[9] and PEsPU from small molecule ester diols, such as triethylene glycol glycolate, lactate, etc., and 2,4-TDI (or MDI),[17,18] all concentrated on the −NH region, and for the −C═O absorption, no effort was made due to the various possible interaction patterns.

It is interesting to resolve the complicated carbonyl absorption bands in ester-based polyurethanes. In this study, we attempted to evaluate the H-bond interactions between urethane and two types of ester linkages (external and internal esters as shown in Figure 1). As illustrated in Figure 1, there are four types of H-bond interactions. In order to resolve all the possible interaction pairs, four model compounds (U_s, U_u, UE_{ex}, and UE_{in} in Scheme 1) with inherent urethane or/and ester groups were prepared and their thermal properties and IR spectra investigated. As suggested from the above reports, emphasis on the effect of thermal treatment is necessary since the carbonyl absorption is closely related to the physical structures of the test samples. Therefore, differential scanning calorimetry (DSC) and X-ray diffraction were employed to evaluate the physical structures of the model compounds. The IR spectra were then studied in terms of the thermal history of the test samples. The results from model compounds can be therefore applied to the polymer cases. With this regard, two polyurethanes (PU_1 and PU_2 in Scheme 2), with either external or internal ester groups, were prepared and their IR spectra were resolved on the basis of the results from model studies. The liquid crystalline PU_2 has its IR spectra investigated in the solid, mesomorphic, and isotropic liquid states. Similar to the model compounds, qualitative views of all carbonyl absorptions were examined in terms of their morphological changes.

Results and Discussion

Four model compounds, U_s, U_u, UE_{ex}, and UE_{in}, and two polymers, PU_1 and PU_2, were prepared according to Schemes 1 and 2, respectively. Reaction of 1-butanol (or 1-pentanol) with 2,4- (or 2,6-) TDI yielded compound U_u (or U_s). In an analogous manner, compound EU_{ex} (or EU_{in}) was prepared by the condensation reaction of 2,4-TDI with the corresponding precursor, 5-hydroxypentyl benzoate (HB) (or *p*-(2-hydroxyethyl)phenylene benzoate (HPB)). The precursor was prepared by reacting excess hydroxyl compound (pentanediol or *p*-(2-hydroxyethyl)phenol (HP)) with benzoyl chloride. For the preparations of PU_1 and PU_2, aromatic diol, 1,4-bis(5-hydroxypentyl) terephthalate (BHPT) (or 1,4-bis-[*p*-(2-hydroxyethyl)phenylene] terephthalate (BHEPT), was the required precursor and synthesized primarily by the reaction of excess pentanediol (or HP) with terephthaloyl chloride. The diol BHPT (or BHEPT) was then condensed with 2,4-TDI to yield the polyurethane, PU_1 (or PU_2).

Model compounds U_u and U_s were used to study the H-bond interactions between urethane −C═O and −NH. EU_{ex} and EU_{in}, with their inherent external and internal ester groups, can be used to study the ester−urethane and urethane−urethane interactions. Furthermore, polymers PU_1 and PU_2 were prepared to demonstrate the complicated interactions derived from ester (either external or internal esters) and urethane linkages. In either the model compounds or polymers, the morphological changes are fundamentally important for the IR study; therefore, investigation on the effect of thermal history is primarily required.

Primary Investigation on Model Compounds. Symmetric and unsymmetric model compounds, U_s and U_u, showed different behaviors under inspection by DSC. The as-reacted U_s exhibited its melting endotherm at around 175 °C (Figure 2a). The fast crystallization rate of U_s can be confirmed by the presence of the crystallization exotherm in the immediate cooling run (Figure 2b). The unsymmetric U_u showed a different crystallization behavior. In the first heating run, it showed a melting endotherm at a lower temperature of 81 °C (Figure 2c) as compared to U_s; however, no

Scheme 1. Syntheses of Model Compounds, U_s, U_u, UE_{in}, and UE_{ex}

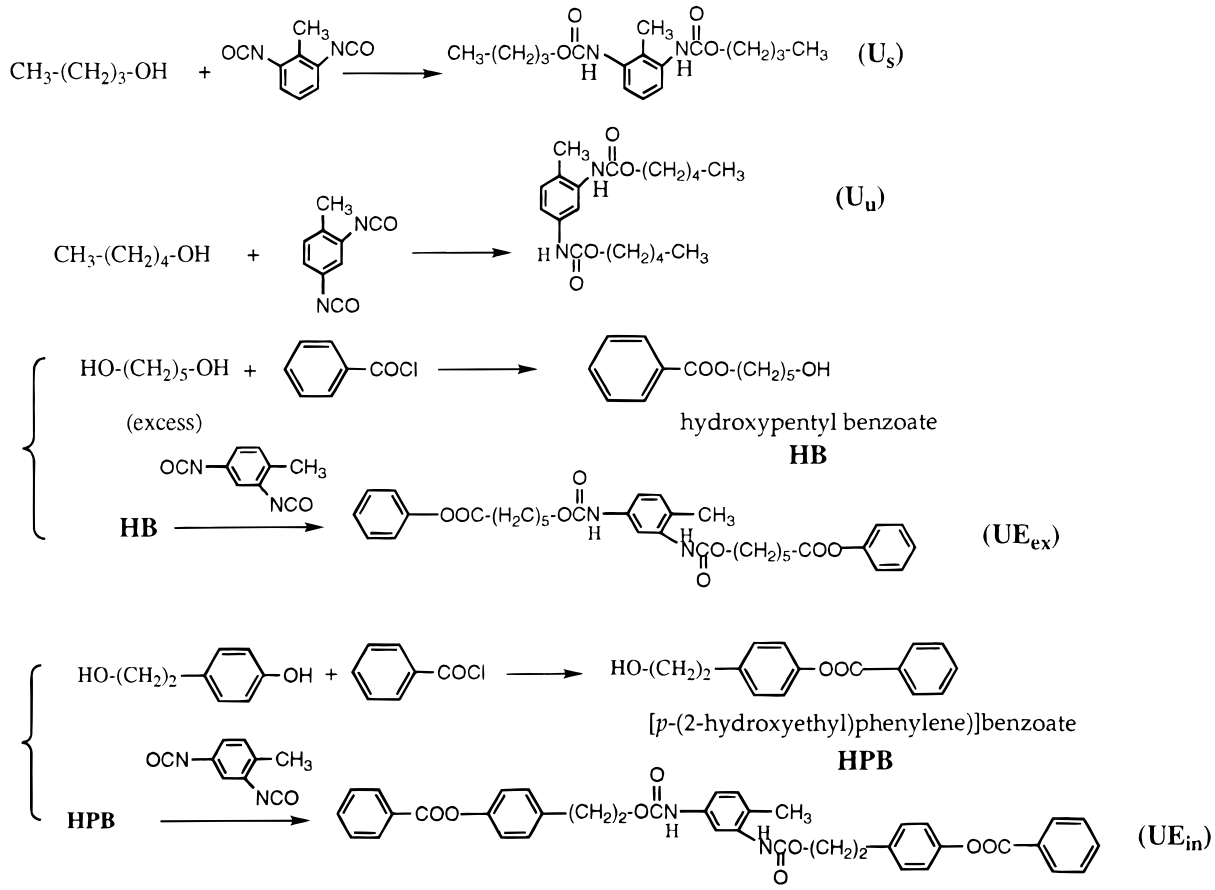

Scheme 2. Syntheses of PU_1 and PU_2

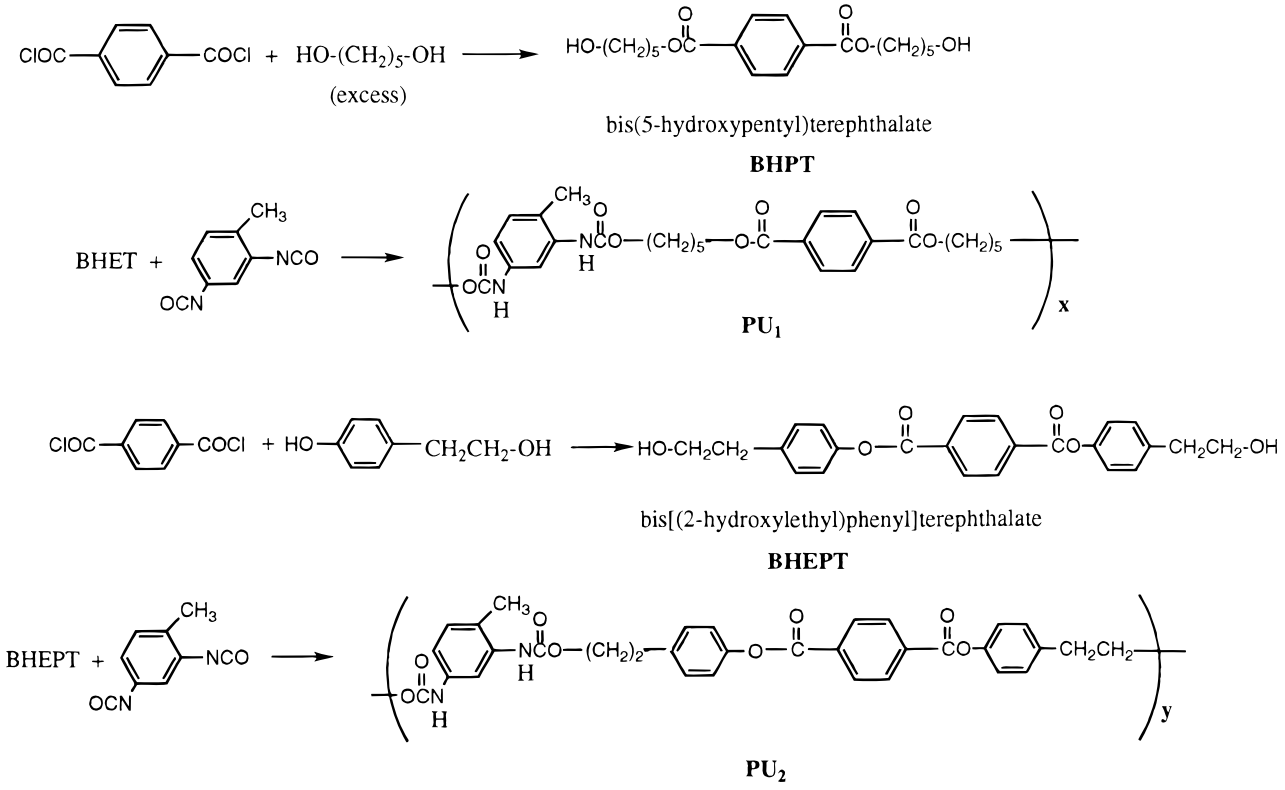

crystallization exotherm can be observed in the corresponding cooling curve (Figure 2d). The melting endotherm can be regenerated if the heat-treated U_u was kept at room temperature for 2 days. It is suggested that the crystalline structure of the as-reacted U_u was induced by the solvent used at the synthesis stages. Compound U_s, with the symmetrical structure derived from 2,6-TDI, is supposed to have a higher crystallization rate as compared to U_u, which has an unsymmetric kink derived from 2,4-TDI.

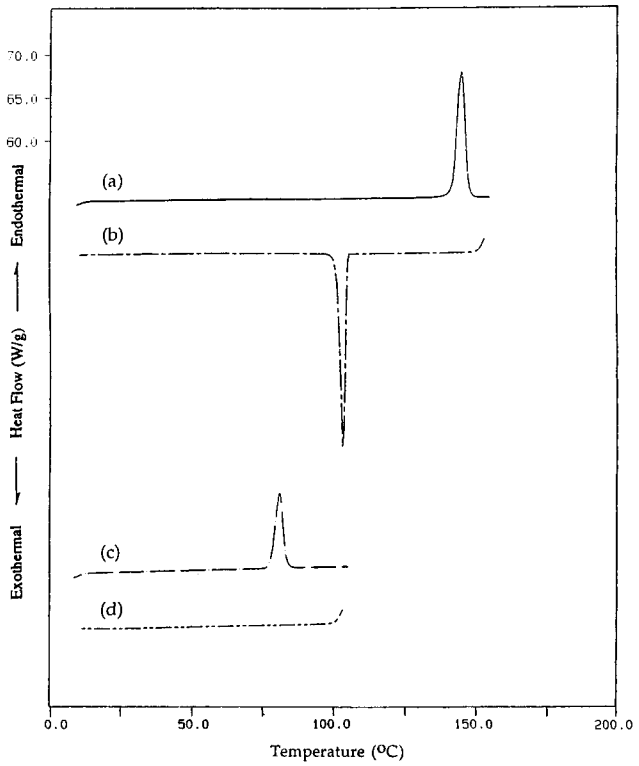

Figure 2. DSC thermograms of (a) the as-reacted U_s in the first heating run, (b) U_s in the cooling run from the melt, (c) the as-reacted U_u in the first heating run, and (d) U_u in the cooling run from the melt (heating and cooling rates = 20 °C/min).

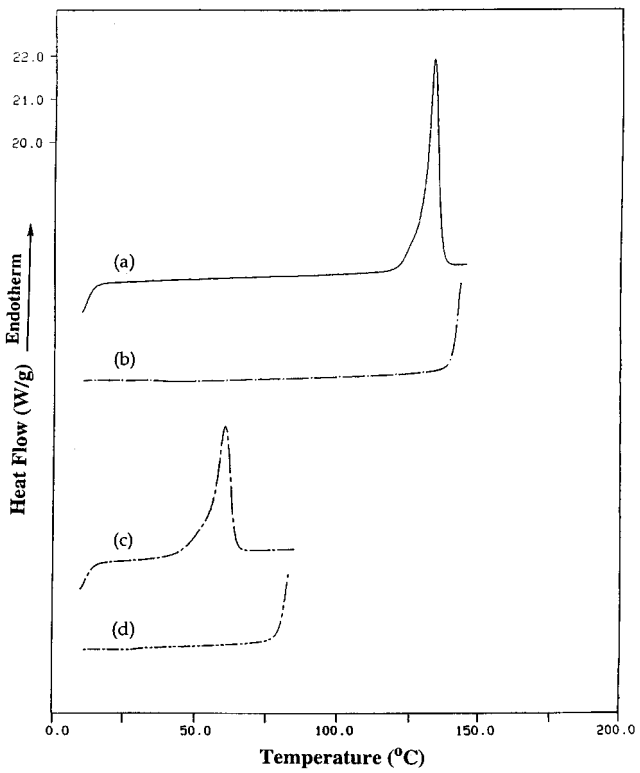

Figure 3. DSC thermograms of (a) the as-reacted UE_{in} in the first heating run, (b) UE_{in} in the cooling run from the melt, (c) the as-reacted UE_{ex} in the first heatig run and, (d) UE_{ex} in the cooling run from the melt.

In contrast to U_s and U_u, the crystalline structures in the as-reacted UE_{ex} and UE_{in} are difficult to be regenerated once samples were heated to melt (cf. Figure 3). Both UE_{in} and UE_{ex} exhibited no sign of crystallization, as samples were immediately cooled from the molten states. Continuous effort by keeping the heat-treated samples at room temperature for 3 days still resulted in the absence of crystalline melting. As compared to U_s and U_u, compounds EU_{ex} and EU_{in} have larger molecule sizes and more complicated interaction patterns due to their inherent ester and urethane linkages. These two factors are supposed to retard the arrangement of the molecular chains in a regular manner.

Selected X-ray diffraction patterns of U_u and UE_{ex} are shown in Figure 4. As consistent with the DSC results, the samples lost the crystalline diffraction peaks appearing in the as-reacted samples (Figure 4b vs 4a and 4e vs, 4d) once they were heated to melt. For U_u, the sharp crystalline diffraction peaks, although with some variations, could be regenerated as the heat-treated sample was further annealed at room temperature for 2 days, while for UE_{ex}, the featureless diffraction pattern, as shown in Figure 4e, still remained even after prolonged annealing at room temperature. The same observation was achieved in the case of UE_{in}.

IR Spectra of Model Compounds. All IR spectra for model compounds were given in the −NH and −C═O absorption regions. As suggested by the DSC results, the as-reacted and heat-treated samples may have different IR absorption patterns in these two regions. The as-reacted U_s exhibited single and narrow −NH and −C═O absorptions bands centered at 3288 and 1694 cm^{-1} (Figure 5a), respectively. The sharp peak shape and the frequencies for both −NH and −C═O absorptions suggested that most of the urethane groups in the U_s are H-bonded. After heat treatment, both bands basically remained intact (except a slight broadening; cf. Figure 5a,b). This result certainly referred to the high crystallization rate as suggested by the DSC study. The as-reacted U_u (Figure 6a) showed a narrow −NH stretching at 3298 cm^{-1} and two sharp −C═O absorption bands at 1714 and 1694 cm^{-1}, respectively. After heat treatment, the −NH stretching (Figure 6b) became broader and shifted to ahigher frequency, and a left shoulder attributed to the free urethane −NH appeared at around 3443 cm^{-1}. The shift in position of the band maximum to higher frequency corresponds to a reduction on the average strength of the hydrogen bonds. This frequency shift and emergence of the $-NH_{free,u}$ band suggested a less-ordered structure was introduced by thermal treatment. The two −C═O absorptions at 1714 and 1694 cm^{-1} for the as-reacted U_u had been previously assigned to be disordered and ordered bonded carbonyl ($-C{=}O_{bonded,u}$) absorptions,[5] respectively. These two resolvable −C═O absorptions broadened and became inseperable (Figure 6b) once U_u was heated to melt. The broad −C═O absorption band can be deconvoluted into three peaks centered at 1733, 1716, and 1700 cm^{-1}, respectively. The peak at 1733 cm^{-1} is due to the free urethane −C═O ($-C{=}O_{free,u}$) while the two low-frequency ones at 1718 and 1700 cm^{-1} are the disordered and ordered $-C{=}O_{bonded,u}$ absorptions. The emergence of the $-C{=}O_{free,u}$ absorption at 1733 cm^{-1} and the shift of the disordered and ordered $C{=}O_{bonded,u}$ absorptions to higher frequencies all indicate a less ordered structure for the heat-treated as compared to the as-reacted U_u, a result also verified by the study on the −NH absorption region.

The IR spectra of model compounds UE_{in} and UE_{ex} were shown in Figures 7 and 8, respectively. Considering the various H-bond interactions between ester and urethane linkages, a complicated −NH absorption pat-

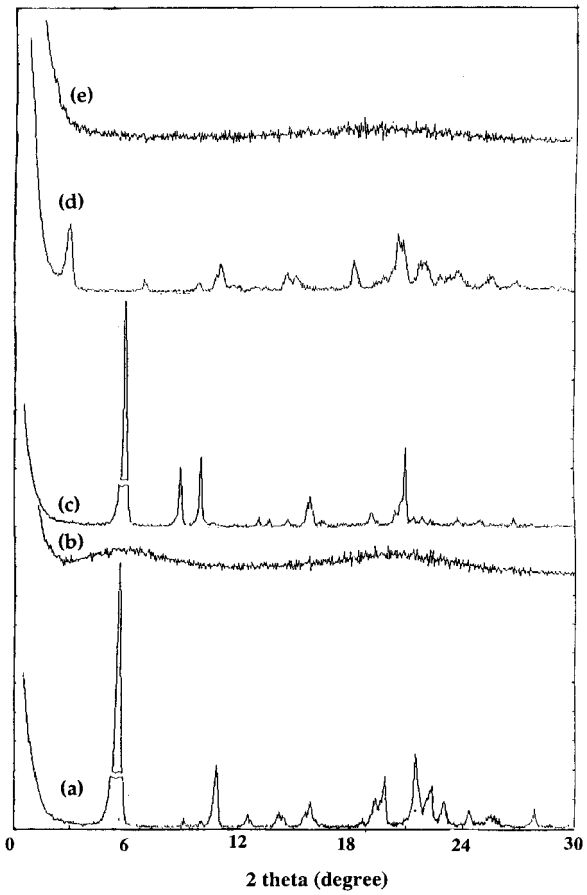

Figure 4. Room temperature X-ray diffraction patterns of (a) the as-reacted U_u, (b) the heat-treated U_u, (c) the heat-treated U_u after being kept at room temperature for 2 days, (d) the as-reacted UE_{ex}, and (e) heat-treated UE_{ex}.

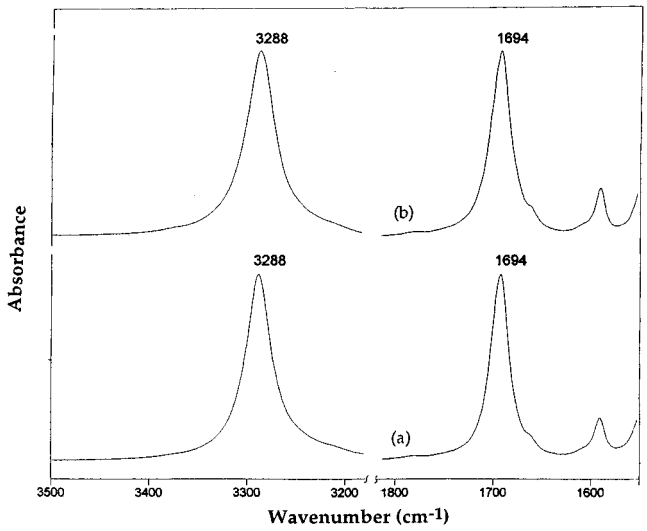

Figure 5. FTIR spectra in the N—H and —C═O stretching regions for (a) the as-reacted U_s and (b) U_s after cooling from the isotropic liquid state.

tern is expected. For both the as-reacted UE_{in} and UE_{ex} (cf. Figures 7a and 8a), an unsymmetric —NH absorption pattern was observed; however, the large left shoulder for UE_{in} (Figure 7a) suggests a high percentage of the —NH groups is situated in a nonbonded conformation. Similar to U_u, the —NH stretchings for both compounds broadened and shifted to higher frequencies as samples were heat-treated (cf. Figures 7b and 8b). Both the as-reacted UE_{in} and UE_{ex} showed a clear, distinct —C═O absorption pattern despite their complicated chemical structures. These —C═O absorptions required further deconvolution and curve-fitting, and the result will be given below. Before that, we also observed the broadening of the —C═O absorptions after heat treatment. This gross change of the peak shape by thermal treatment is similar to the case of U_u.

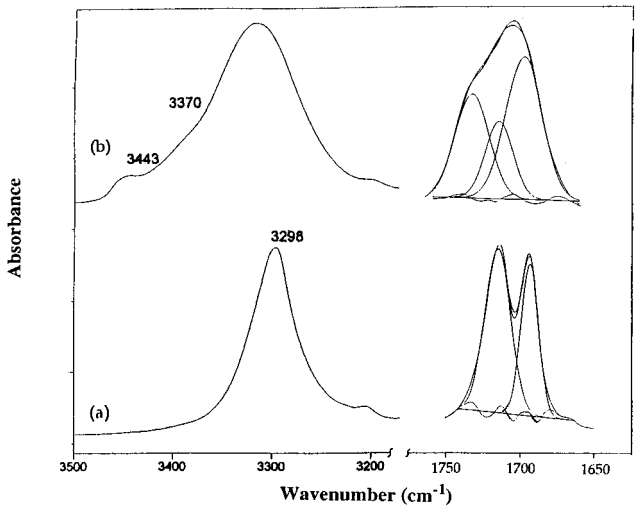

Figure 6. FTIR spectra in the N—H and —C═O stretching regions for (a) the as-reacted U_u and (b) U_u after cooling from the isotropic liquid state.

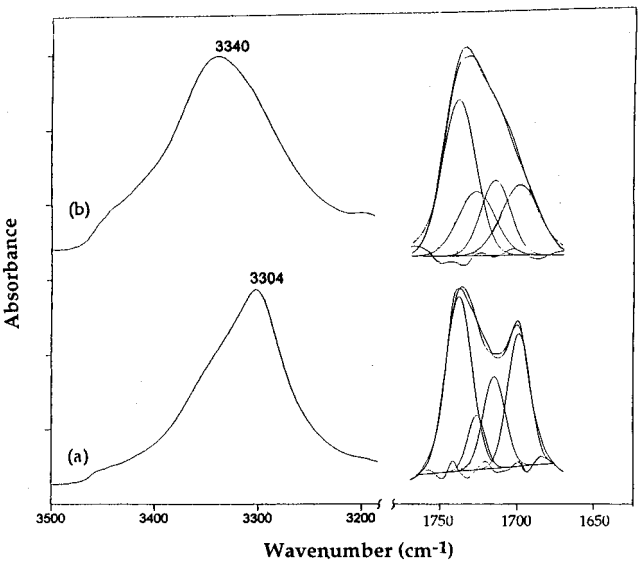

Figure 7. FTIR spectra in the N—H and —C═O stretching regions for (a) the as-reacted UE_{in} and (b) UE_{in} after cooling from the isotropic liquid state.

According to the previous reports on polyamides and polyurethanes,[19—24] the —NH stretchings generally have a strong dependence of their extinction coefficients upon absorption frequencies and this results in the conformational insensitivity of the —NH absorption. Therefore, we concentrated more on the carbonyl absorption region. Table 1 gives the deconvoluted data of the carbonyl absorptions for both the as-reacted and heat-treated model compounds (for comparison, data for U_s and U_u are also included). Before further comment on the deconvoluted results, we should discuss some limitations of the curve-fitting method.

According to the conclusion drawn by Maddams,[19] the number of component peaks in a composite profile and their half-widths are the two most critical variables in the curve-fitting process. The number of component peaks in our system can be reasonably determined on

Table 1. IR Data (cm^{-1}) adapted from the Model Compounds

	ordered −C=O$b_{onded,u}$[b]		disordered −C=O$_{bonded,u}$[c]		−C=O$_{free,u}$[d]		E$_{bonded,ex}$[e]		E$_{free,ex}$[f]		E$_{free,in}$[g]	
compound[a]	υ^h	$W_{1/2}{}^i$	υ^h	$W_{1/2}{}^i$	υ^h	$W_{1/2}{}^i$	υ^h	$W_{1/2}{}^i$	υ^h	$W_{1/2}{}^i$	υ^h	$W_{1/2}{}^i$
as-reacted U_s	1693	22.3										
heat-treated U_s	1693	25.9										
as-reacted U_u	1693	13.8	1715	20.2								
heat-treated U_s	1699	29.0	1715	22.1	1734	27.1						
as-reacted UE_{ex}	1690	11.4	1714	6.9	1730	15.4	1710	15.1	1722	11.7		
heat-treated UE_{ex}	1698	24.5	1717	14.1	1735	23.4	1707	21.5	1723	18.9		
as-reacted UE_{in}	1699	17.1	1715	16.8	1728	13.3					1738	20.3
heat-treated UE_{in}	1698	29.8	1715	22.7	1727	28.2					1738	25.8

[a] KBr pellet was used. [b] Ordered bonded urethane −C=O, referred to the urethane −C=O ortho to the methyl group. [c] Disordered bonded urethane −C=O, referred to the urethane −C=O para to the methyl group. [d] Free urethane −C=O. [e] Bonded external ester −C=O. [f] Free external ester −C=O. [g] Free internal ester −C=O. [h] The frequency of the band maximum. [i] The width at half-height.

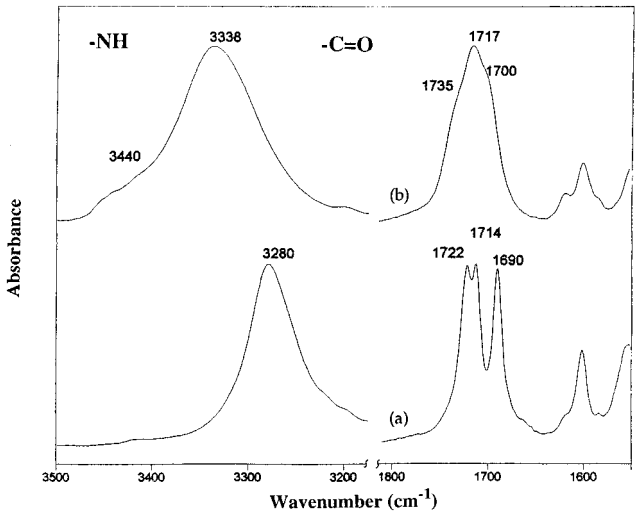

Figure 8. FTIR spectra in the N−H and −C=O stretching regions for (a) the as-reacted UE_{ex} and (b) UE_{ex} after cooling from the isotropic liquid state.

the basis of the possible interactions, which will be discussed below. On the contrary, no proven methods are available for the half-widths of the component peaks for band systems with appreciable overlap. Therefore, reliable values for parameters, such as peak shape and the base line are required to optimize the widths during the curve-fitting calculations. A simple linear base line with its two end points removed from the overlapping peak system was used. For the peak shape, a Gaussian instead of Lorentzian profile was assumed in our fitting procedure. As suggested by Maddams,[19] Lorentzian profiles are generally better than Gaussian approachs; but for closely overlapping peaks, the use of a Gaussian shape may be appropriate. Use of a linear baseline and Gaussian profiles resulted in the respective band frequencies falling in the reasonable ranges reported for urethanes[8,14] (the frequency assignments for the ester groups will be discussed below). The resulting band frequencies are reliable since a deviation on peak frequency assignment for more than 2 cm^{-1} would result in an unacceptable fitting. Nevertheless, some values of the calculated widths are hard to justify. Certain resolved bands in Table 1 (e.g., −C=O$_{free,u}$ and −E$_{free,in}$ for the as-reacted and heat-treated UE_{in}) are too close together and separated by less than half their half-widths. This phenomen is common for a markedly overlapped system; however, uncertain width values would result in an unreliable determination of the peak areas.

The extinction coefficient is another issue to be considered if quantitative analysis of the peak area is considered. Previously, the ratios of extinction coefficients between the H-bonded and nonbonded bands (as ϵ_b/ϵ_f) have been determined.[20, 25−29] The ϵ_b/ϵ_f values obtained from different polyurethanes (or polyamides blends) ranged from 1.05 to 1.8.[20,25−27] For ester systems, the reported ϵ_b/ϵ_f values were based on their interactions with hydroxyl groups.[28,29] No extinction coefficient for a urethane −NH bonded ester −C=O absorption was previously determined due to the scarcity of reliable methodology to monitor the H-bond interaction between ester and urethane groups. Scarce data on extinction coefficients and the uncertainty on the peak aress prohibit a reliable, quantitative analysis. Therefore, no data on the peak areas were listed in Table 1.

According to Table 1, two other bands, in addition to the ordered −C=O$_{bonded,u}$ and −C=O$_{free,u}$ absorptions, had been assigned and attributed to the free and bonded external ester −C=O (−C=O$_{free,ex}$ and −C=O$_{bonded,ex}$) absorptions for the as-reacted UE_{ex}. The assignment for −C=O$_{free,ex}$ can be confirmed from the previous study on an analogous liquid crystalline small molecule,[30] bis[4-((pentyloxy)carbonyl)phenylene] terephthalate ($(CH_3(CH_2)_4OOCC_6H_4OOCC_6H_4COOC_6H_4COO(CH_2)_4CH_3$, BPT)) and other related compounds.[31,32] In the crystalline state, two −C=O$_{free,ex}$ absorptions at 1722 and 1703 cm^{-1} were observed, while in the mesomorphic and isotropic liquid states, the lower absorption due to the dipole−dipole interaction (or the presence of different crystal forms) disappeared and only the peak at 1722 cm^{-1} remained. Therefore, results from BPT support our assignment for the −C=O$_{bonded,ex}$ absorption in UE_{ex}. The failure to observe the 1703 cm^{-1} peak for the as-reacted UE_{ex} indicates a less-ordered crystalline structure of the bulky, unsymmetric UE_{ex} as compared to the symmetric BPT.

To confirm the −C=O$_{bonded,ex}$ absorption frequency, liquid methyl benzoate ($C_6H_5COOCH_3$, MB) with an inherent external ester structure was prepared (cf. Experimental Section) to serve as solvent for U_u and to simulate the H bonds between the urethane −NH and the external ester −C=O groups. The pure MB possesses a characteristic absorption at 1723 cm^{-1} (Figure 9a, the peak at 3424 cm^{-1} is due to the overtone of the ester −C=O). This frequency is due to the −C=O$_{free,ex}$ absorption and close to the values (1722 cm^{-1}) obtained from the solid state IR spectra of BPT and UE_{ex}, as described above. Also, the −C=O$_{free,u}$ absorption at 1735 cm^{-1} in U_u can be obtained from the IR spectrum in CH_2Cl_2. The dilute solution of MB in U_u (Figure 9b; U_u ∼10% of the total weight) exhibited a broader peak centered at 1725 cm^{-1}. Presumably, this peak is a mixed mode contributed from a major −C=O$_{free,ex}$ and other minor carbonyl absorptions, which can be further verified by the concentrated solution. As the concentra-

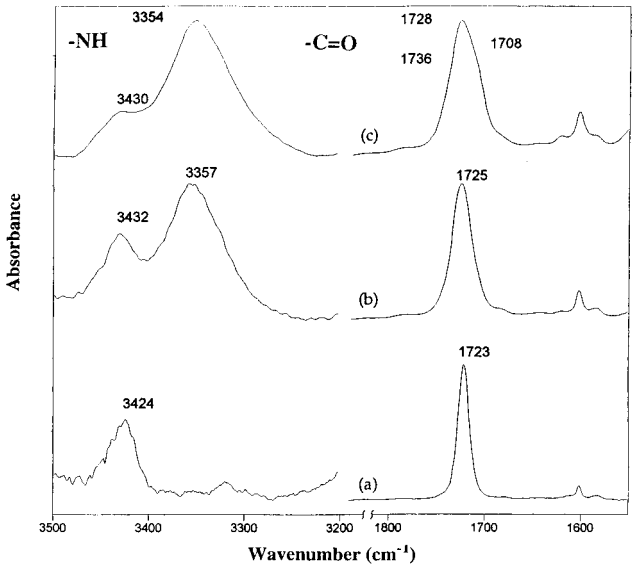

Figure 9. FTIR spectra in the N—H and −C═O stretching regions for (a) the puremethyl benzoate (MB, the peak at 3424 cm^{-1} is the overtone of −C═O), (b) the dilute solution of U_s in MB (10 wt %), and (c) the concentrated solution of U_s in MB (15 wt %).

tion of the U_u (U_u ~15% of the total weight) is increased, three peaks at 1736, 1726, and 1708 cm^{-1} can be resolved according to the deconvolution method (Figure 9c). The peak at 1726 cm^{-1} is due to the $-C{=}O_{free,ex}$ absorption according to the spectrum of pure MB. The peak at 1736 cm^{-1} can be easily identified to be the $-C{=}O_{free,u}$ absorption. Therefore, the peak at 1708 cm^{-1} is considered to be generated from the remaining possibility, the bonded external ester ($-C{=}O_{bonded,ex}$). Since both solutions possess low U_u concentrations, the urethane −NHs in U_u are either nonbonded or bonded to the external ester −C═O in the surrounding MB (bonding to urethane −C═O is limited). The 1708 cm^{-1} (or 1707 cm^{-1} for UE_{ex}) peak is therefore originated from the $-C{=}O_{bonded,ex}$ group.

Another noticeable IR result in Table 1 is the absence of the bonded internal ester carbonyl absorption for UE_{in}. To prove it, diphenyl terephthalate (DPT) was intentionally prepared (cf. Experimental Section) and mixed with equal amounts of model U_s. The corresponding solid-state IR absorption in the −C═O region (Figure 10) showed the presence of two resolvable Gaussian-shape peaks centered at 1732 ($-C{=}O_{free,in}$) and 1693 cm^{-1} (ordered $-C{=}O_{free,u}$), respectively. The failure to observe any other −C═O absorption may prove the incapability of the internal −C═O to bond with urethane −NH, which resulted in one less −C═O peak for UE_{in} as compared to UE_{ex} (cf. Table 1). This result can be explained by the steric reason. For UE_{in}, the two bulky phenylene units in the neighborhood of the internal esters shield the sandwiched −C═O units from the reach of the other intermolecular urethane −NH groups. Analogous result for the incapability of the internal ester −C═O to bond with the hydroxyl proton had been previously disclosed in our laboratory.[30] Liquid crystalline bis[4-(((5-hydroxypentyl)oxy)carbonyl)phenylene] terephthalate ($HO(CH_2)_5OOCC_6H_4$-$OOCC_6H_4COOC_6H_4COO(CH_2)_5OH$, BHPPT) can form an interdigitated smectic A mesophase due to the intermolecular H-bonding between the −OH terminals and the external ester −C═O groups, but no structure generated from interaction between the −OH and the internal ester −C═O was found according to the X-ray diffraction result. The incapability of the −OH groups

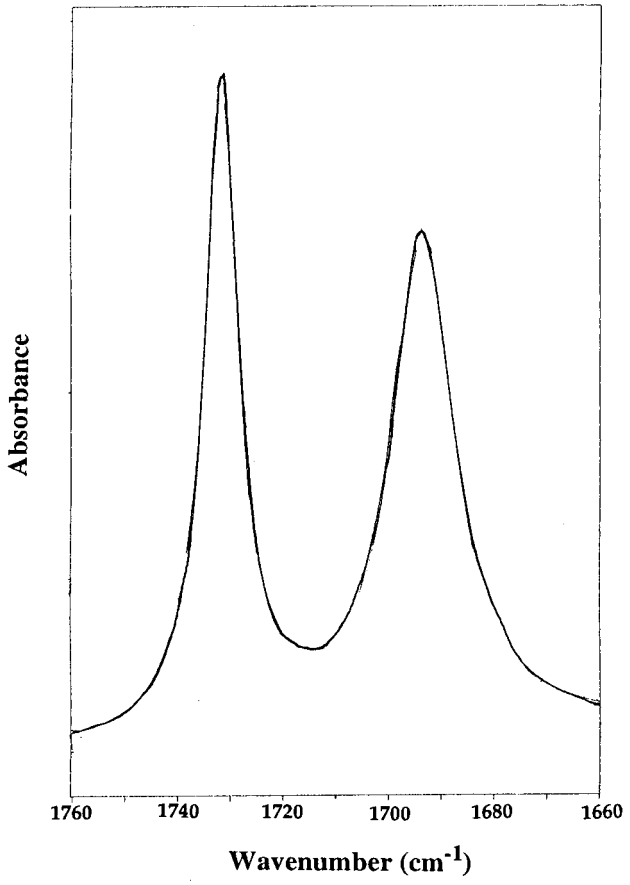

Figure 10. FTIR absorption of the solid mixtures of DPT and U_u (1:1 by weight) in the −C═O region (KBr pellet).

to form H-bonds with the internal ester −C═O in BHPPT may suggest the same situation for the urethane −NHs in UE_{in}. Also, this argument can be intensified in view of the steric reason. The urethane −NHs in UE_{in} are connected to the aromatic phenylene ring and therefore, more sterically impossible to form H-bonds with internal esters than the −OHs in BHPPT, which are directly linked to a flexible aliphatic chain.

According to Table 1, a few more observations can be given here. Firstly, heat-treatment also resulted in the broadening of the respective peak (as indicated by the increased value of width at the half-height, $W_{1/2}$). This suggests that thermal treatment disrupted the ordered structure in the as-reacted samples. However, this peak broadening is limiting for the ordered $-C{=}O_{bonded,u}$ absorption of the symmetric U_s. The minor thermal effect is reasonable in considering the minor difference between the as-reacted and heat-treated U_s suggested by DSC study. Actually, the ordered $-C{=}O_{bonded,u}$ band generally had the most significant shift upon heat treatment (cf. U_u and UE_{ex} in Table 1). In the case of U_u, the shift of the ordered $-C{=}O_{bonded,u}$ band was accompanied by the emergence of the $-C{=}O_{free,u}$ absorption at 1734 cm^{-1}. For UE_{ex}, the shifts of the band frequencies include the $-C{=}O_{bonded,u}$, the $-C{=}O_{free,u}$, and $-C{=}O_{bonded,ex}$ bands. Thermal treatment interrupted the structure in the ordered (crystalline) domain, which should consequently influence the free and bonded carbonyl environment at the same time and temporally (or ultimately) transform this structure into a less-ordered one. In contrast to U_u and UE_{ex}, the respective band maximum frequencies remained intact for compound UE_{in} irrespective of the thermal treatment (the difference between the as-reacted and heat-treated UE_{in}

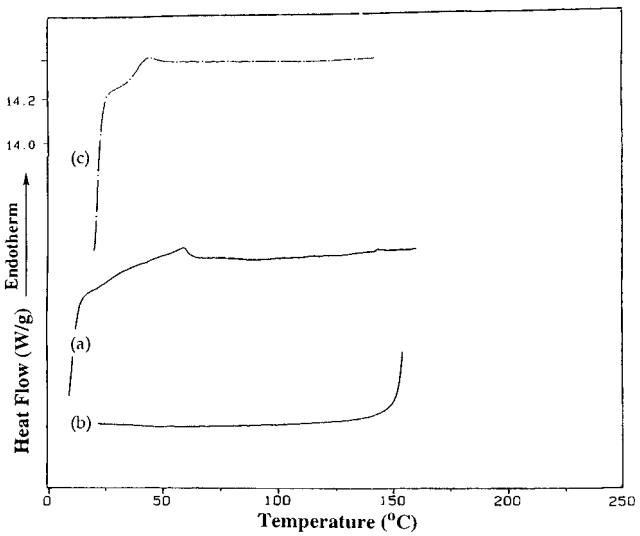

Figure 11. DSC thermograms of PU_1 in (a) the first run, (b) the cooling run after heating to 160 °C, and (c) the second heating run after (b) (heating and cooling rates = 20 °C/min).

is the width at half-height, $W_{1/2}$). This result is related to the chemical structure of UE_{in}. It is proposed that the two terminal bulky diads make UE_{in} less susceptible to thermal agitation. Transformation from crystalline to fluid states intensified the motions of the chain segments in UE_{in}, but the environments around the carbonyl groups remained approximately the same between these two states. This is contrast to UE_{ex}, which possesses less bulky phenylene terminals.

Qualitative Study on PU_1 and PU_2. Polyurethanes PU_1 and PU_2 were designed and prepared to qualitatively confirm the results from model compounds. PU_1 is amorphous in nature, as indicated by its DSC thermograms (Figure 11), which showed only the glass transition in the first and the second runs. The kink structure derived from the 2,4-TDI moiety and the capability of the external ester −C═O, in addition to urethane −C═O, to bond with the urethane −NH would interfere with a regular packing pattern generally existing in homopolyurethanes and result in the amorphous structure In contrast, PU_2 is a liquid crystalline material due to its mesogenic triad structure. At temperatures below 150 °C, PU_2 has its glass transition at around 80 °C followed by several small endotherms, which are due to certain crystallization processes, as will be further identified below. This as-reacted PU_2 showed its melting endotherm at 172 °C (crystal to mesophase, T_m) and isotropization transition (T_i) in the range of 200−225 °C (Figure 12a). The second heating after cooling from 250 °C resulted in the significant glass transition at a temperature higher than that of the first heating scan and a small melting transition at 168 °C (Figure 12b). A slow crystallization rate was suggested as PU_2 was cooled from the isotropic liquid state. However, this melting transition could be largely recovered (Figure 12c) if PU_2, after cooling from the mesophase (205 °C), was subsequently heated at 150 °C ($> T_g$) for 3 h. The solvent-induced crystallinity of the as-reacted PU_2 was mostly destroyed in the first heating run to the isotropic liquid state. Annealing at a temperature higher than T_g would successfully induce crystallization from the amorphous sample cooled from the mesophase. Under polarized light, PU_2 exhibited an uncharacteristic texture at 180 °C (Figure 13). To confirm the mesophase, PU_2 was further examined by X-ray diffraction (Figure 14). The as-reacted PU_2

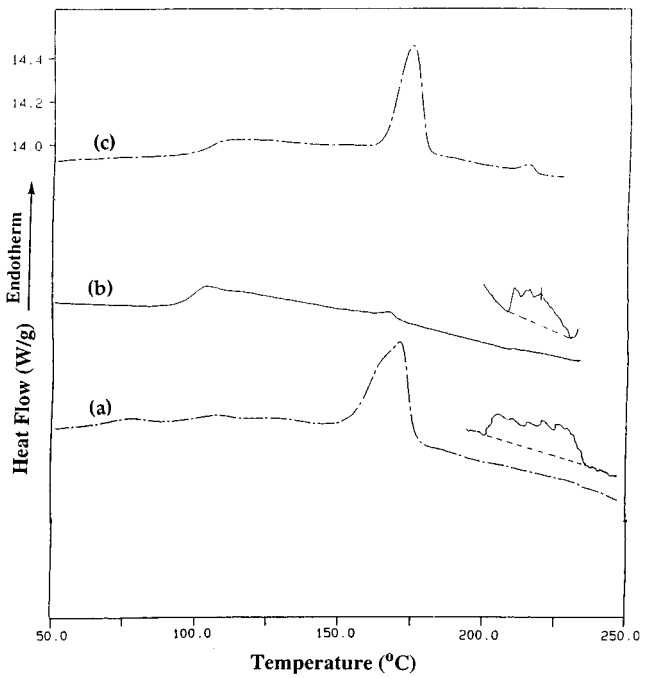

Figure 12. DSC thermograms of PU_2 in (a) the first run, (b) the seoncd run after cooling from 250 °C (isotropic liquid state), and (c) the second heating run after cooling from 205 °C (mesomorphic state) and annealing at 150 °C for 3 h (heating rate = 20 °C/min).

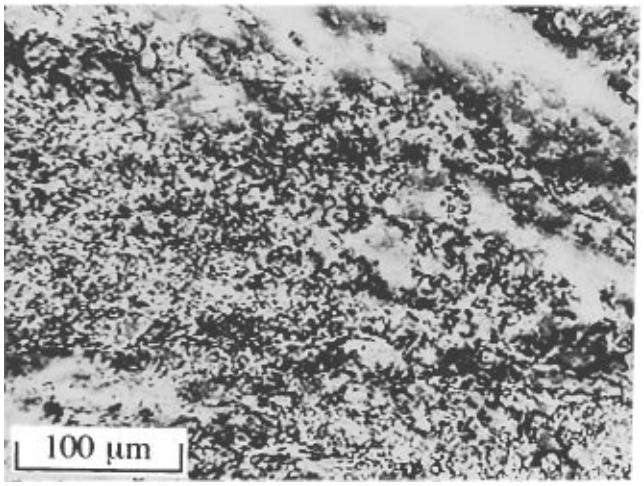

Figure 13. POM photograph of PU_2 at 180 °C.

showed several small crystalline diffraction peaks imposed on the amorphous backgrounds. As PU_2 was further heated to temperatures above T_g (i.e., 120 and 145 °C), several sharp crystalline diffraction peaks (as indicated by the arrows) emerged in the high-angle region (in the 2θ range 18−22°; corresponding to an intermolecular distance of 3−5 Å) . Concurrently, the diffraction peaks in the low-angle region ($2\theta \sim 6°$) became diffuse and broad, indicating the decrease of the long-range order (or the presence of a large crystalline domain). Supposedly, the increase of the crystallinity in the high-angle region is due to the enhancement of the intermolecular packing in the amorphous or the small crystalline domains. The crystalline diffraction peaks disappeared as PU_2 was transformed into the mesomorphic state (i.e., at 175 °C). At 175 °C, the broad peak pattern in the range 2θ = 18−22° indicates a nematic mesophase for PU_2. The featureless pattern remained intact as long as PU_2 was heated above T_i.

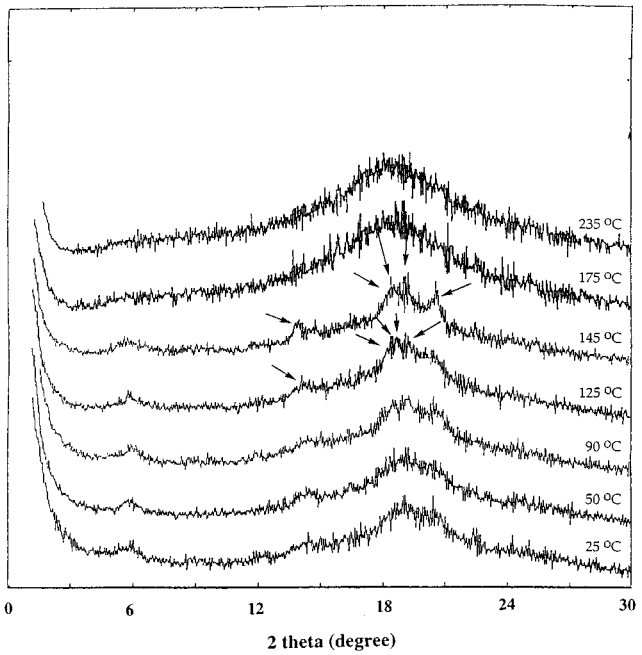

Figure 14. X-ray diffraction patterns of PU_2 at different temperatures. (Arrows indicate the emergence of the crystalline diffraction peaks at elevated temperatures.)

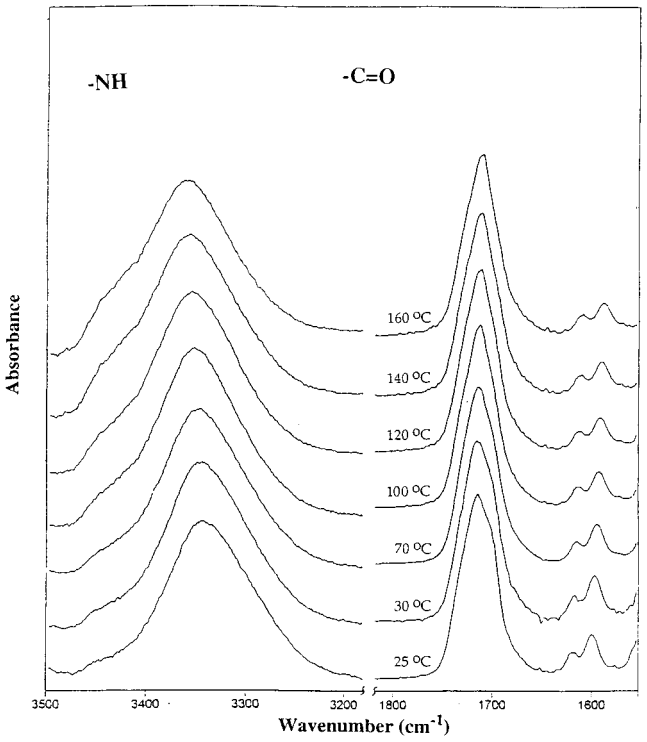

Figure 15. FTIR spectra in the N−H and −C═O stretching regions for PU_1 at different temperatures.

The IR spectra of PU_1 and PU_2 were given in Figures 15 and 16, respectively. The IR spectra of PU_1 at different temperatures are basically the same except the −NH band maximum shifted with temperature, which is reasonable since the average strength of the −NH bond should be decreased with increasing thermal motion. As consistent with the DSC result, the broad absorption patterns suggest both the as-reacted and heat-treated PU_1 are amorphous in nature (actually, its −C═O absorption pattern is similar to the amorphous polyurethane prepared from hexanediol and 2,4-TDI[14]). In contrast, there are major changes for the PU_2 sample

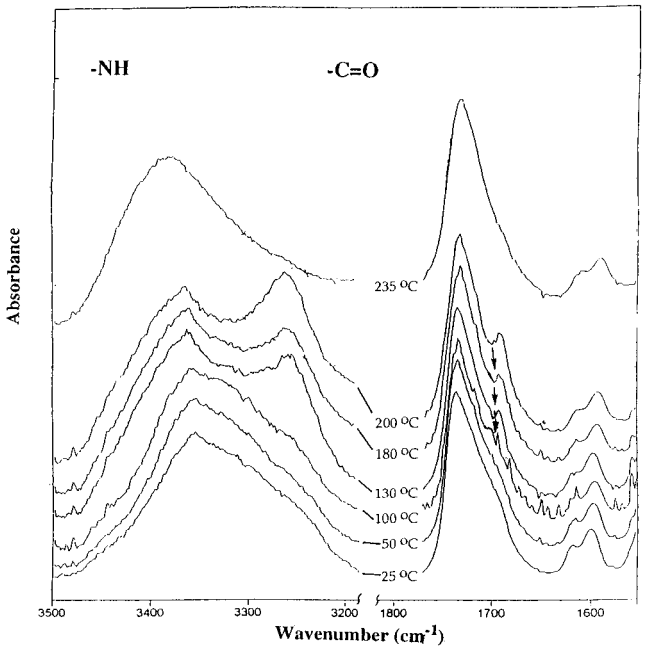

Figure 16. FTIR spectra in the N−H and −C═O stretching regions for PU_2 at different temperatures.

(cf. Figure 16). Firstly, the original broad −NH absorption transformed into two resolvable peaks once the sample was heated to 130 °C. Since the study on UE_{in} suggested that the internal esters are unable to bond with urethane −NHs, the −NH variations for PU_2 should be mainly attributed to the urethane−urethane interactions. Disregarding the dependence of the −NH extinction coefficient on temperature, the abrupt increase of the bonded −NH absorption at around 3270 cm^{-1} is related to the formation of a more ordered (crystalline) domain at temperatures $> T_g$. This observation is consistent with the X-ray diffraction study illustrated above. These two-peaks remained intact in the mesophase range but merged into one broad one once the sample was heated to the isotropic liquid state. Secondly, the −C═O absorption gradually changed its peak shape as the temperature was increased. The as-reacted PU_2 exhibited a broad, unsymmetric −C═O absorption pattern at 25 and 50 °C. Correlated with the −NH absorption, increasing the temperature to 130 °C resulted in the emergence of the 1692 cm^{-1} peak (as indicated by the arrow). There are other small changes on the absorption shape, which should be further analyzed by the deconvolution and curve-fitting procedures. Beforehand, we should realize these variations are basically caused by the transformations between T_g, T_m (melting temperature), and T_i (isotropization temperature) as described by the DSC and X-ray diffraction.

The deconvoluted results from Figures 15 and 16 were summarized in Table 2. The amorphous PU_1 was assigned on the basis of the data obtained from the heat-treated UE_{ex}, while for PU_2, both data from the as-reacted and heat-treated UE_{in} were used, dependent on the temperature (or the physical state) discussed. For PU_1, the inertness of the ordered $-C{=}O_{bonded,u}$ peak frequency (and the other absorption frequencies listed in Table 2) suggested that no major structure change can be achieved by thermal treatment, a result consistent with the DSC experiment. In contrast, the peak frequency of the ordered $-C{=}O_{bonded,u}$ for PU_2 changed from 1699 to 1691 cm^{-1} and the width at half-height ($W_{1/2}$, changed from 32.5 to 23.4 cm^{-1}) reduced as the sample was heated to 180 °C, a variation coherent with

Table 2. IR Data (cm^{-1}) Adapted from PU_1 and PU_2

	ordered $-C=O_{bonded,u}$[b]		disordered $-C=O_{bonded,u}$[c]		$-C=O_{free,u}$[d]		$E_{bonded,ex}$[e]		$E_{free,ex}$[f]		$E_{free,in}$[g]	
compound[a]	υ^h	$W_{1/2}{}^i$	υ^h	$W_{1/2}{}^i$	υ^h	$W_{1/2}{}^i$	υ^h	$W_{1/2}{}^i$	υ^h	$W_{1/2}{}^i$	υ^h	$W_{1/2}{}^i$
as-reacted PU_1	1698	34.7	1716	17.4	1734	21.8	1708	21.0	1723	16.4		
heat-treated PU_1	1698	32.5	1716	27.6	1734	22.7	1707	19.1	1722	17.1		
as-reacted PU_2	1699	32.5	1718	20.5	1732	17.9					1740	23.5
PU_2 (175 °C)	1691	23.4	1716	21.7	1728	13.7					1738	23.0
heat-treated PU_1	1699	31.6	1717	23.8	1731	19.0					1739	24.0

[a] Polymer film was applied. [b] Ordered bonded urethane −C═O, referred to the urethane −C═O ortho to the methyl group. [c] Disordered bonded urethane −C═O, referred to the urethane −C═O para to the methyl group. [d] Free urethane −C═O. [e] Bonded external ester −C═O. [f] Free external ester −C═O. [g] Free internal ester −C═O. [h] The frequency of the band maximum. [i] The width at half-height.

the pattern change in the −NH region. The shift of the ordered $C=O_{bonded,u}$ to lower frequencies and the reduction of the peak width indicate the formation of a more ordered structure in the mesophase. The −C═O absorption patterns in the mesophase (i.e., 180 °C) are approximately the same as those at 130 °C (a state between T_m and T_g), while the result from X-ray diffraction indicates the change of the short-range order. The macroscopically different domains may have identical spectroscopic features, which supports the fact that the state between T_g and T_m has segmental microstructures similar to those in the mesomorphic state. Again, as similar to the −NH absorption, the −C═O absorption became diffuse as PU_2 was heated to the isotropic liquid state and no more pattern change could be observed with any further thermal treatments.

The variations on chain conformations of PU_2 between different states can be conceptually depicted. The kink introduced by the 2,4-TDI unit caused the low crystallinity of the as-reacted PU_2. As the semicrystalline PU_2 was heated to temperatures above T_g, the increasing chain mobility enhanced the intermolecular packing in the small crystalline domains and increased the crystallinity. As PU_2 was transformed into the mesomorphic state, the crystalline domains were melted but the stiff chain segments and the orientation order maintained the chain packing arranged in a manner similar to that of the solid state between T_g and T_m, as suggested from the IR result. Further heating transformed the ordered mesophase into the isotropic liquid state, whose randomness was indicated by the broadenings of both the −NH and −C═O absorption bands and caused the reduction of the average strength of the −NH bonds. However, this gross change may be due to the urethane exchange reactions or the accompanied decomposition (a separate isothermal TGA study at 235 °C suggested a slight weight loss (∼ 3 wt %) occurred after 30 min).

Conclusion

Model compounds of U_s, U_u, UE_{in}, and UE_{ex} were synthesized to resolve the IR spectra of the homopolyurethanes of PU_1 and PU_2. With the inherent kink structure introduced by the 2,4-TDI, U_u, UE_{in}, and UE_{ex} are more difficult to recrystallize than the symmetric U_s. Accordingly, the −C═O absorptions of U_u, UE_{in}, and UE_{ex} are affected by the thermal history. The −C═O absorption patterns from both the as-reacted and heat-treated samples were compared and deconvoluted into the constituent peaks (cf. Table 1). Generally, a heat-treated sample possesses a broader peak as compared to an as-reacted one. Also, the more ordered samples possess lower absorption frequencies as compared with the less ordered samples. Among all peaks, the ordered $-C=O_{bonded,u}$ absorption showed a more drastic shift of peak frequency toward thermal treatment than other absorption modes. A study on UE_{ex} and UE_{in} revealed that the external ester −C═O can bond with urethane −NH while for the internal ester −C═O, no absorption corresponding to bonded groups was detected. This difference may be attributed to the bulky environment around the internal esters.

IR spectra of homopolyurethane PU_1 can be interpreted on the basis of the results from the less-ordered, heat-treated UE_{ex}. No major difference was observed between the as-reacted and heat-treated UE_{ex} since both of them are amorphous in nature. In addition to the kink in the main chain and the low aromaticiy of PU_1, interactions between the external ester and urethane would interrupt the regular packing generally encountered in normal polyurethanes and result in the amorphous structure of PU_1. In contrast, the inherent rigid, mesogenic triads introduced the mesomorphic state for PU_2. At temperatures higher than T_g, the as-reacted PU_2 reorganized to increase its crystallinity. The resulting crystalline structures subsequently melted into a nematic mesophase. The IR study suggests that the orientation order in the mesophase keeps the H-bond behavior approximately the same as in the semicrystalline state between T_g and T_m. Curve-fitting of PU_2 in the mesomorphic state was based on the more ordered, as-reacted UE_{in} while those in the solid and isotropic liquid states were on the assigned frequencies for the heat-treated UE_{in}. The result also suggests that a drastic frequency shift for the ordered $-C=O_{bonded,u}$ absorption occurred as PU_2 was heated into the mesomorphic state.

Experimental Section

Materials and Instrumentation. All the solvent distillations were performed under a nitrogen atmosphere. Methylene chloride for IR spectroscopy (Tedia, 99.9%) was distilled from its mixture with calcium hydride and stored over molecular sieves 4 Å (Linde). Tetrahydrofuran (THF) was distilled from a mixture of sodium and benzophenone and used immediately after distillation. *N*,*N*-Dimethylforamide (DMF) was vacuum distilled after dehydration with barium oxide. 1,1,2,2-Tetrachloroethane (TCE; Showa, >95%) was predried over molecular sieves 4 Å for at least 2 weeks before use. Benzoyl chloride (TCI, >99%) and terephthaloyl chloride (TCI, >99%) were recrystallized from *n*-hexane. *n*-Pentanol (TCI, >98%), *n*-butanol (TCI, >98%), and 1,5-pentanediol (TCI, >97%) were vacuum dried at 50 °C for 12 h and stored over molecular sieves 4 Å (Linde).

Proton NMR spectra were recorded with a Varian Femini-200 200 MHz model. Tetramethylsilane (TMS) was used as the internal standard in all cases. Biorad FTS-40 and FTS-155 Fourier transform infrared spectrometers were used. Spectra in the optical range of 4000−400 cm^{-1} were obtained by averaging 64 scans at a resolution of 2 cm^{-1}. A KBr pellet was used for the solid samples, and a liquid cell with a KBr window, for liquid samples. In order to analyze the carbonyl absorption, deconvolution and curve-fitting were employed to resolve it into several constituents. For a logic approach, the corresponding carbonyl absorption was smoothed and a linear

baseline was determined before deconvolution was made. The curve-fitting was made on the basis of the following principles: Firstly, the number of the different carbonyl absorption modes was determined on the basis of the possible interaction patterns in the corresponding model compounds and polyurethanes. The band shapes of the free and bonded urethane, and ester ones, were then assumed to be Gaussian. Curve-fitting is limited to the spectral data of the carbonyl region between 1770 and 1660 cm^{-1}, where a linear base line was assumed. In all cases, a two-stage fitting process was applied to approximate the correctness of the inital parameters chosen. The procedures afford a best-fit of the original curve and the resulting correlation factor for all the fittings are over 0.995. Textures of liquid crystals were observed with a Nikon Optiphot-POL microscope equipped with a Linkam TMS controller and a THMS 600 hot stage. Phase transition temperatures were detected with a Perkin-Elmer DSC 7 model. The carrier gas was nitrogen at a flow rate of ca. 10 mL/min. Calibration of the calorimeter was conducted for each heating rate using an indium standard. X-ray diffraction was performed with a Siemens Diffraktometer D 5000 model with Ni-filtered Kα radiation.

Synthesis. The general synthesis procedures of model compounds and polymers were described in Schemes 1 and 2, respectively. In addition, two other compounds, methyl benzoate (MB) and diphenyl terephthalate (DPT), were prepared in order to identify certain IR absorption frequencies. All the details were given below.

Synthesis of Methyl Benzoate, MB. A solution of benzoyl chloride (15 g; 107 mmol) in CH_2Cl_2 (20 mL) was added dropwise to vigorously stirred methanol (50 mL; 1232 mol). The reaction mixture was refluxed for 8 h under a nitrogen atmosphere. The hot solution was filtered and the filtrate was subjected to rotary evaporation to remove most of the solvent. The crude product was then dissolved in $CHCl_3$ and subjected to two-phase extraction with aqueous $NaHCO_3$ (pH = 7) once and saturated aqueous NaCl twice. The organic layer was dried over $MgSO_4$, filtered, and concentrated. The resulting oily liquid is the final product. R_f = 0.87 (ethyl acetate/*n*-hexane = 1:2 v/v). ^{1}H NMR (200 MHz, $CDCl_3$): δ 8.06−8.02 (d, 2 H, aromatic Hs ortho to $-COOCH_3$), 7.55 (t, 1 H, J = 8 Hz, aromatic H para to $-COOCH_3$), 7.42 (t, 2 H, J = 8 Hz, aromatic Hs meta to $-COOCH_3$), 3.90 (s, 3 H, $-COOCH_3$).

Synthesis of Diphenyl Terephthalate, DPT. A solution of terephthaloyl chloride (1.5 g; 7.4 mmol) in CCl_4 (20 mL) was added slowly to mechanically stirred mixtures of phenol (2.1 g; 15 mmol) and 0.1 N aqueous NaOH (160 mL). To ensure the complete dissolution, more aqueous NaOH (30 mL) was added at this time. The reaction was performed at room temperature for 6 h. The white solid was filtered out and washed with 0.01 N aqueous NaOH (500 mL). The resulting solid was further washed with distilled water and dried in the vacuum oven to obtain final product. R_f = 0.84 (ethyl acetate/*n*-hexane = 1:2 v/v). Anal. Calcd for $C_{20}H_{14}O_4$: C, 75.46; H, 4.43. Found: C, 75.52; H, 4.38. ^{1}H NMR (200 MHz, $CDCl_3$): δ 8.33 (s, 4 H, $-OCOC_6H_4COO-$), 7.45 (t, 4 H, J = 8 Hz, aromatic Hs meta to −O−), 7.37 (t, 2 H, J = 8 Hz, aromatic Hs para to −O−), 7.22 (d, 4 H, aromatic Hs ortho to −O−).

Synthesis of Model Compound, U_s. To a nitrogen-blanketed solution of 5-pentanol (10 mL, 92.1 mmol) in THF (10 mL), a solution of 2,6-TDI (0.5 mL, 3.5 mmol) in THF (5 mL). The reaction mixture was refluxed for 12 h, and then a catalytic amount of dibutyltin dilaurate (ca. 0.5 wt %) was added. The reaction was continued for another 12 h and then cooled to room temperature before rotary evaporation to remove the residual solvent. The resulting mixture was subjected to two-phase extraction with $H_2O/CHCl_3$ several times. The organic layer was then dried over $MgSO_4$ and filtered. The filtrate was concentrated before the addition of *n*-hexane to precipitate the white powder. This crude product was subjected to Soxhlet extraction with *n*-hexane overnight. The final product was obtained by precipitation from $CHCl_3$/*n*-hexane twice and vacuum evacuation at 50−55 °C for 24 h. Mp = 141 °C. R_f = 0.68 (ethyl acetate/*n*-hexane = 1:3 v/v). Anal. Calcd for $C_{19}H_{30}N_2O_4$: C, 65.12; H, 8.63; N, 7.99. Found: C, 65.18; H, 8.46; N, 8.03. ^{1}H-NMR (200 MHz, DMSO-d_6): δ 8.86 (s, 2 H, $-NHCOO-$), 7.19−7.04 (m, 3 H, aromatic H), 4.03 (t, 4 H, J = 6 Hz, $-COOCH_2-$), 2.03 (s, 3 H, toluenyl $-CH_3$), 1.60 (t, 4 H, J = 6 Hz, $-OCH_2CH_2-$), 1.32 (m, 8 H, $-OCH_2CH_2CH_2CH_2-$), 0.89 (t, 6 H, J = 6 Hz, $-CH_2CH_3$).

Synthesis of Model Compound, U_u. Preparation procedures are identical to those operated for compound U_s as described above; however, purification procedures after Soxhlet extraction were different. The crude product was first eluted with ethyl acetate/*n*-hexane (=1:2 v/v), and then precipitated from $CHCl_3$/*n*-hexane twice, filtered, and dried at for 24 h. Anal. Calcd for $C_{17}H_{26}N_2O_4$: C, 63.33; H, 8.13; N, 8.69. Found: C, 63.49; H, 8.07; N, 8.88. R_f = 0.72 (ethyl acetate/*n*-hexane = 1:2 v/v). ^{1}H-NMR (200 MHz, DMSO-d_6): δ 9.49 (s, 1 H, $-OCONH-$ para to the toluenyl $-CH_3$), 8.74 (s, 1 H, $-OCONH-$ ortho to the toluenyl $-CH_3$), 7.49 (s, 1 H, aromatic H), 7.17−7.13 (d, 1 H, aromatic H), 7.06−7.02 (d, 1 H, aromatic H), 4.05 (t, 4 H, J = 6 Hz, $-COOCH_2-$), 2.11 (s, 3 H, toluenyl $-CH_3$), 1.66−1.52 (m, 4 H, $-COOCH_2CH_2-$), 1.46−1.28 (m, 4 H, $-COOCH_2CH_2CH_2-$), 0.91−0.87 (t, 6 H, J = 8 Hz, $-CH_2CH_3$).

Synthesis of Model Compound, UE_{ex}. Solution of benzoyl chloride (4 g; 28.5 mmol) in TCE (20 mL) was added slowly to a vigorously stirred solution of 1,5-pentanediol (80 mL; 760 mmol) in THF (40 mL). The reaction mixture was then heated at 80 °C for 8 h under a nitrogen atmosphere. The residual solvent was removed by rotary evaporation, and $CHCl_3$ was added to redissolve the mixture. The resulting solution was subjected to two-phase extraction with aqueous $NaHCO_3$ (pH = 7) once and saturated aqueous NaCl twice. The organic layer was dried over $MgSO_4$, filtered, and concentrated. A powder of 5-hydroxypentyl benzoate was obtained after precipitation from *n*-butane once and $CHCl_3$/*n*-hexane twice.

To a nitrogen-blanketed solution of 5-hydroxypentyl benzoate (2 g; 9.6 mmol) in DCE (10 mL) was slowly added 2,4-TDI (0.66 mL, 4.6 mmol). The reaction mixture was heated at 80 °C for 12 h and then a catalytic amount of dibutyltin dilaurate (ca. 0.5 wt%) was added. The reaction was then continued for another 12 h. The resulting solution was concentrated before addition of *n*-hexane to precipitate the crude product. The white powder was continually extracted with *n*-hexane overnight. The final product was obtained by precipitation from $CHCl_3$/*n*-hexane twice and vacuum evacuation at 50−55 °C for 24 h. Mp = 62 °C. Anal. Calcd for $C_{23}H_{38}N_2O_8$: C, 67.10; H, 6.48; N, 4.74. Found: C, 67.10; H, 6.49; N, 4.87. R_f = 0.50 (ethyl acetate/*n*-hexane = 1/2 v/v). ^{1}H-NMR (200 MHz, DMSO-d_6): δ 9.52 (s, 1 H, $-OCO-NH-$ para to the toluenyl $-CH_3$), 8.77 (s, 1 H, $-OCONH-$ ortho to the toluenyl $-CH_3$), 7.99−7.95 (d, 4 H, aromatic Hs in the benzoyl ring), 7.65 (t, 2 H, J = 8 Hz, aromatic Hs in the benzoyl ring), 7.51 (t, 4H, J = 8 Hz, aromatic Hs in the benzoyl ring), 7.50 (s, 1 H, aromatic H in the toluene ring), 7.18−7.13 (d, 1 H, aromatic H in the toluene ring), 7.06−7.02 (d, 1 H, aromatic H in the toluene ring), 4.29 (t, 4 H, J = 6 Hz, $-COOCH_2-$), 4.08 (t, 4 H, J = 6 Hz, $-NHCOOCH_2-$), 2.10 (s, 3 H, toluenyl $-CH_3$), 1.83−1.62 (m, 8 H, $-COOCH_2CH_2CH_2CH_2CH_2-$OCONH−), 1.57−1.44 (m, 4 H, $-COOCH_2CH_2CH_2-$).

Synthesis of Model Compound, UE_{in}. A solution of 4-(2-hydroxyethyl)phenol (6 g; 43.4 mmol) in 0.4 N aqueous NaOH (110 mL) was added slowly to a solution of benzoyl chloride (6 g; 42.7 mmol) in TCE (20 mL). The mixture was stirred at room temperature for 8 h and extracted with aqueous $NaHCO_3$ (pH = 7) twice and saturated aqueous NaCl solution once. The resulting organic layer was dried over $MgSO_4$ and filtered. The filtrate was concentrated and the crude product was precipitated from *n*-hexane. The resulting powder was precipitated from $CHCl_3$/*n*-hexane twice, filtered, and vacuum dried at 50−55 °C for 12 h to obtain the product *p*-(2-hydroxyethyl)-phenylene benzoate.

A solution of *p*-(2-hydroxyethyl)phenylene benzoate (2 g; 8.3 mmol) in DCE (20 mL) was added to a solution of 2,4-TDI (0.6 mL; 40.2 mmol) in DCE (3 mL) under a nitrogen atmosphere. The reaction mixture was heated at 80 °C for 12 h before the addition of dibutyltin dilaurate (ca. 0.5 wt %). The reaction was continued for another 12 h. The reaction mixture was then concentrated, and *n*-hexane was added to precipitate the crude product. The product was further subjected to Soxhlet

extraction with *n*-hexane overnight and precipitated from $CHCl_3$/*n*-hexane twice. The final product was obtained by vacuum evacuation at 50−55 °C for 24 h. Mp = 133 °C. Anal. Calcd for $C_{39}H_{34}N_2O_8$: C, 71.11; H, 5.20; N, 4.25. Found: C, 71.11; H, 5.32; N, 4.37. R_f = 0.44 (ethyl acetate/*n*-hexane = 1/2 v/v). ^{1}H-NMR (200 MHz, DMSO-d_6): δ 9.57 (s, 1 H, −OCON*H*− para to the toluenyl −CH_3), 8.85 (s, 1 H, −OCON*H*− ortho to the toluenyl −CH_3), 8.15−8.11 (d, 4 H, aromatic Hs in the benzoyl ring), 7.75 (t, 2 H, J = 8 Hz, aromatic Hs in the benzoyl ring), 7.60 (t, 4H, J = 8 Hz, aromatic Hs in the benzoyl ring), 7.49 (s, 1 H, aromatic H in the toluene ring), 7.40−7.36 (d, 4 H, aromatic Hs in −OC_6H_6−), 7.24−7.20 (d, 4 H, aromatic Hs in −OC_6H_6−), 7.20−7.16 (d, 1 H, aromatic H in the toluene ring), 7.08−7.04 (d, 1 H, aromatic H in the toluene ring), 4.30 (t, 4 H, J = 8 Hz, −NHCOOCH_2−), 2.97 (t, 4 H, J = 6 Hz, −$C_6H_6CH_2CH_2$−), 2.10 (s, 3H, toluenyl −CH_3).

Synthesis of Polyurethane from Bis(5-hydroxypentyl) Terephthalate (BHPT)/2,4-TDI. A mixture of 1,5-pentanediol (80 mL; 760 mmol) and THF (40 mL) was added slowly to a solution of terephthaloyl chloride (4.1 g; 20.0 mmol) in CCl_4 (30 mL). The solution was then stirred at room temperature for 8 h. The resulting mixture was then concentrated and subjected to two-phase extraction ($CHCl_3$/$NaHCO_3$ (pH = 7)). The excess 1,5-pentanediol was removed by the addition of saturated. The organic layer was dried over $MgSO_4$ and filtered, and most of the solvent was rotariy evaporated before precipitating with *n*-hexane. The resulting solid was redissolved in $CHCl_3$ and precipitated from *n*-hexane. The above procedure was performed twice. The final product of 1,4-bis(5-hydroxypentyl) terephthalate was obtained by vacuum evacuation at 40 °C for 24 h.

A solution of bis(5-hydroxypentyl) terephthalate (2 g; 5.9 mmol) in THF (40 mL) was added slowly into a solution of 2,4-TDI (0.87 mL; 6.1 mmol) in THF (3 mL). The reaction was performed at 70 °C for 24 h before the addition of dibutyltin dilaurate (ca. 0.5 wt %). The reaction was then continued for another 36 h before the addition of methanol to quench the reaction. The reaction solvent was removed by rotary distillation. The resulting solid was redissolved in THF, and the solution was slowly added into methanol to precipitate the polymer. The above procedure was performed twice. The final product was obtained by drying at 40 °C for 24 h. ^{1}H NMR (200 MHz, DMSO-d_6): δ 9.49 (s, 1 H, −OCON*H*− para to toluene ring), 8.73 (s, 1 H, −OCON*H*− ortho to the toluene ring), 8.05 (s, 4 H, −$OCOC_6H_4COO$−), 7.51 (s, 1 H, aromatic H in the toluene ring), 7.14−7.10 (d, 1 H, aromatic H in the toluene ring), 7.03−6.99 (d, 1 H, aromatic H in the toluene ring), 4.29 (b, 4 H, −$C_6H_4COOCH_2$−), 4.06 (b, 4 H, −NHCOOCH_2−), 2.08 (s, 3 H, toluenyl −CH_3), 1.78−1.64 (m, 8 H, −$COOCH_2CH_2CH_2CH_2CH_2CH_2OCONH$−), 1.58−1.46 (m, 4 H, −$COOCH_2CH_2CH_2$−). η_{inh} (35.0 ± 0.05 °C in TCE) = 0.22 dL/g.

Synthesis of Polyurethane from Bis[*p*-(2-hydroxyethyl)phenyl] Terephthalate (BHEPT)/2,4-TDI, PU_2. A solution of *p*-(2-hydroxyethyl)phenol (20.8 g; 150 mmol) in 0.4 N aqueous NaOH (400 mL) was added slowly into a solution of benzoyl chloride (15.3 g; 75 mmol) in CCl_4 (100 mL). The mixture was stirred at room temperature for 6 h, and the white solid was filtered off. Further extraction was made with aqueous $NaHCO_3$ (pH = 7) solution and saturated salt water. The organic layer was separated, dried over $MgSO_4$, and filtered. The final product of [1,4-bis(2-hydroxyethyl)phenylene] terephthalate was obtained by recrystallization from ethyl acetate twice. Mp = 243 °C.

Solution of [1,4-bis(2-hydroxyethyl)phenylene] terephthalate (1.2 g; 3.0 mmol) in THF (80 mL) was added to a mixture of 2,4-TDI (0.44 mL; 3.1 mmol) in THF (5 mL) under a nitrogen atmosphere. The reaction mixture was refluxed for 12 h before the addition of dibultyltin dilaurate (ca. 0.5 wt %). The reaction was continued for another 36 h and then methanol was added to terminate the reaction. The reaction mixture was concentrated and *n*-hexane was added to precipitate the crude product. The white powder was redissolved in THF and added dropwise to methanol to precipitate the crude product. The final product was obtained by vacuum evacuation at 50−55 °C for 24 h. ^{1}H NMR (200 MHz, DMSO-d_6): δ 9.57 (s, 1 H, −OCON*H*− para to the toluenyl −CH_3), 8.56 (s, 1 H, −OCON*H*− ortho the toluenyl −CH_3), 8.31 (s, 4 H, −$OCOC_6H_4$-COO−), 7.50 (s, 1 H, aromatic meta H in the toluene ring), 7.42−7.38 (d, 4 H, aromatic Hs in −$C_6H_4CH_2CH_2$−), 7.29−7.25 (d, 4 H, aromatic Hs in −$C_6H_4CH_2CH_2$−), 7.20−7.16 (d, 1 H, aromatic H in the toluene ring), 7.08−7.04 (d, 1 H, aromatic H in the toluene ring), 4.31 (b, 4 H, −NHCOOCH_2−), 2.99 (b, 4 H, −$C_6H_4CH_2CH_2$−), 2.11 (s, 3 H, toluenyl −CH_3). η_{inh} (35.0 ± 0.05 °C in TCE) = 0.13 dL/g.

Acknowledgment. This work was financially supported by The National Science Council, ROC, under contract number NSC84-2216-E-110-008.

References and Notes

(1) *Multiphase Polymers*; Cooper, S. L., Estes, G. M., Eds; Advances in Chemistry Series 176; American Chemical Society: Washington, DC, 1979.
(2) Coleman, M. M.; Garf, J. F.; Painter, P. C. *Specific Interactions and the Miscibility of Polymer Blends*; Technomic Publishing Co.: Lancaster, PA, 1991.
(3) Hummel, D. O.; Ellinghorst, G.; Khatchatryan, A.; Stenzenberger, F. D. *Angew. Makromol. Chem.* **1979**, *82*, 129.
(4) Boyarchuk, Y. M.; Rappoport, L. Y.; Nikitin, V. N.; Apukhtine, N. P. *Polym. Sci. USSR* **1965**, *7*, 859.
(5) Sung, C. S. P.; Schneider, N. S. *Macromolecules* **1975**, *8*, 68.
(6) Pollack, S. K.; Smyth, G.; Papadimitrakopoulos, F.; Stenhouse, P. J.; Hsu, S. L.; MacKnight, W. J. *Macromolecules* **1992**, *25*, 2381.
(7) Sung, C. S. P.; Schneider, N. S. *Macromolecules* **1975**, *8*, 68.
(8) Pollack, S. K.; Shen, D. Y.; Hsu, S. L.; Wang, Q.; Stidham, H. D. *Macromolecules* **1989**, *22*, 551.
(9) Lee, J. B.; Kato, T.; Yoshida, T.; Uryu, T. *Macromolecules* **1993**, *26*, 4989.
(10) Tang, W.; MacKnight, W. J.; Hsu, S. L. *Macromolecules* **1995**, *28*, 4284.
(11) Miller, J. A.; Lin, S. B.; Kirk, K. S.; Hwang, K. K. S.; Wu, K. S.; Gibson, P. E.; Cooper, S. L. *Macromolecules* **1985**, *18*, 32
(12) Lee, H. S.; Wang, Y. K.; Hsu, S. L. *Macromolecules* **1987**, *20*, 2089
(13) Yoon, S. C.; Ratner, B. D. *Macromolecules* **1988**, *21*, 2392.
(14) Pollack, S. K.; Smyth, G.; Papadimitrakopoulos, F.; Stenhouse, P. J.; Hsu, S. L.; MacKnight, W. J. *Macromolecules* **1992**, *25*, 2381.
(15) Zharkov, V. V.; Strikovsky, A. G.; Verteleskaya, T. E. *Polymer* **1993**, *34*, 938.
(16) Goddard, R. J.; Cooper, S. L. *Macromolecules* **1995**, *28*, 1390.
(17) Zochniak, A. *J. Appl. Polym. Sci.* **1977**, *21*, 1869.
(18) Zochniak, A. *J. Appl. Polym. Sci.* **1978**, *22*, 215.
(19) Maddams, W. F. *Appl. Spectroscopy* **1980**, *34*, 245.
(20) Coleman, M. M.; Lee. K. H.; Skrovanck, D. J.; Painter, P. C. *Macromolecules* **1986**, *19*, 2149.
(21) Skrovanek, D. J.; Painter, P. C.; Coleman, M. M.; Lee. K. H. *Macromolecules* **1986**, *19*, 699.
(22) Skrovanek, D. J.; Howe, S. E.; Painter, P. C.; Coleman, M. M. *Macromolecules* **1985**, *18*, 1676.
(23) Coleman, M. M.; Skrovanek, D. J.; Howe, S. E.; Painter, P. C. *Macromolecules* **1985**, *18*, 299.
(24) Papadimitrakopoulos, F.; Sawa, E.; MacKnight, W. J. *Macromolecules* **1992**, *25*, 4682.
(25) Seymour, R. W.; Estes, G. M.; Cooper, S. L. *Macromolecules* **1970**, *3*, 579.
(26) Senich, G. A.; MacKnight, W. J. *Macormolecules* **1980**, *13*, 106.
(27) Bhagwager, D. E.; Painter, P. C.; Coleman, M. M.; Krizan, T. D. *J. Polym. Sci., Polym. Phys.* **1991**, *29*, 1547.
(28) Moskala, E. J.; Howe, S. E.; Painter, P. C.; Coleman, M. M. *Macromolecules* **1984**, *17*, 1671.
(29) Garton, A. *Polym. Eng. Sci.* **1984**, *24*, 112.
(30) Lin, C. H.; Hong, J. L; Yen, F. S.; Hong, J. L. *Liq. Cryst.* **1996**, *21*, 609.
(31) Galbiati, E.; Zerbi, G.; Benedetti, E.; Chiellini, E. *Polymer* **1991**, *32*, 1555.
(32) Galbiati, E.; Zoppo, M. D.; Tieghi, G.; Zerbi, G. *Polymer* **1993**, *34*, 1806.

MA970898L